

Enhanced Stability of a Protein with Increasing Temperature

Joachim M. Vinther,[†] Søren M. Kristensen, and Jens J. Led^{*}

Department of Chemistry, University of Copenhagen, Universitetsparken 5,
DK-2100 Copenhagen Ø, Denmark

Received June 20, 2010; E-mail: led@kiku.dk

Abstract: The unusual stability of a structured but locally flexible protein, human growth hormone (hGH) at pH 2.7, was investigated using the temperature dependence of the nanosecond–picosecond dynamics of the backbone amide groups obtained from ¹⁵N NMR relaxation data. It is found that the flexibility of the backbone of the helices decreases with temperature in the range from 24 °C to ~40 °C, corresponding to an increasing stability. A concomitant increase with temperature of the electrostatic interactions between charged residues forming an interhelical network of salt bridges at the center of the four-helix core suggests that these interactions give rise to the decreasing flexibility and increasing stability of the protein. However, numerous hydrophobic interactions in the interior of the four-helix core may also contribute. Above ~40 °C, where the thermal energy overcomes the electrostatic and hydrophobic interactions, a substantial increase in the flexibility of the helix backbones results in a highly positive contribution from the local conformational heat capacity, $C_{p, conf}$, of the helix backbones to the total heat capacity, C_p , of the protein. This reduces the change in heat capacity upon unfolding, ΔC_p , increases the change in the Gibbs free energy, ΔG_{unfold} , and stabilizes the protein at high temperatures. A similar decrease in flexibility is found near other salt bridges in hGH and in Calmodulin and may be of general importance for the thermostability of proteins and, in particular, of the salt bridge intensive thermophilic proteins.

Introduction

Flexibility and stability are crucial for the function of proteins. Although a detailed mapping of these properties still remains a challenge, protein backbone dynamics on the nanosecond–picosecond time scale provides a sensitive probe for studying specific changes in protein flexibility and stability related to the chemical or physical state of the proteins. This has been demonstrated by numerous studies, since the model-free approach^{1,2} and the reduced spectral density mapping method^{3–6} were introduced and proven useful for characterizing the nanosecond–picosecond dynamics of proteins from NMR relaxation rates^{7–9} (see also a recent review by Jarymowycz and Stone¹⁰). In particular, the model-free approach has provided insight into the local flexibility of proteins and its temperature dependence in terms of squared order parameters S^2 of the backbone N–H bond vectors,

the local conformational entropies, S_{conf} , and the local conformational heat capacities, $C_{p, conf}$.^{11–14}

In nearly all NMR studies of protein dynamics so far, backbone order parameters with negative temperature dependencies have been determined,^{14–23} corresponding to local conformational entropies of the backbone N–H vectors that increase with temperature and, thereby, positive contributions to the local conformational heat capacities (see eqs 2 and 3 in the Materials and Methods). Only in a study of a calmodulin–peptide complex²⁴ was a small but significant positive temperature

[†] Present address: Department of Chemistry, Aarhus University, DK-8000 Aarhus, Denmark.

- (1) Lipari, G.; Szabo, A. *J. Am. Chem. Soc.* **1982**, *104*, 4546–4559.
- (2) Lipari, G.; Szabo, A. *J. Am. Chem. Soc.* **1982**, *104*, 4559–4570.
- (3) Farrow, N. A.; Zhang, O.; Forman-Kay, J. D.; Kay, L. E. *Biochemistry* **1995**, *34*, 868–878.
- (4) Peng, J. W.; Wagner, G. *Biochemistry* **1995**, *34*, 16733–16752.
- (5) Ishima, R.; Nagayama, K. *J. Magn. Reson., Ser. B* **1995**, *108*, 73–76.
- (6) Lefèvre, J. F.; Dayie, K. T.; Peng, J. W.; Wagner, G. *Biochemistry* **1996**, *35*, 2674–2686.
- (7) Kay, L. E.; Torchia, D. A.; Bax, A. *Biochemistry* **1989**, *28*, 8972–8979.
- (8) Clore, G. M.; Driscoll, P. C.; Wingfield, P. T.; Gronenborn, A. M. *Biochemistry* **1990**, *29*, 7387–7401.
- (9) Palmer, A. G.; Rance, M.; Wright, P. E. *J. Am. Chem. Soc.* **1991**, *113*, 4371–4380.
- (10) Jarymowycz, V. A.; Stone, M. J. *Chem. Rev.* **2006**, *106*, 1624–1671.

- (11) Akke, M.; Bruschweiler, R.; Palmer, A. G. *J. Am. Chem. Soc.* **1993**, *115*, 9832–9833.
- (12) Li, Z.; Raychaudhuri, S.; Wand, A. *Protein Sci.* **1996**, *5*, 2647–2650.
- (13) Yang, D.; Kay, L. E. *J. Mol. Biol.* **1996**, *263*, 369–382.
- (14) Yang, D.; Mok, Y. K.; Forman-Kay, J. D.; Farrow, N. A.; Kay, L. E. *J. Mol. Biol.* **1997**, *272*, 790–804.
- (15) Mandel, A. M.; Akke, M.; Palmer, A. G. *Biochemistry* **1996**, *35*, 16009–16023.
- (16) Evenas, J.; Forsen, S.; Malmendal, A.; Akke, M. *J. Mol. Biol.* **1999**, *289*, 603–617.
- (17) Spyropoulos, L.; Lavigne, P.; Crump, M. P.; Gagne, S. M.; Kay, C. M.; Sykes, B. D. *Biochemistry* **2001**, *40*, 12541–12551.
- (18) Seewald, M. J.; Pichumani, K.; Stowell, C.; Tibbals, B. V.; Regan, L.; Stone, M. J. *Protein Sci.* **2000**, *9*, 1177–1193.
- (19) Wand, A. *J. Nat. Struct. Biol.* **2001**, *8*, 926–931.
- (20) Pawley, N. H.; Nicholson, S. K. L. *J. Mol. Biol.* **2002**, *324*, 991–1002.
- (21) Vugmeyster, L.; Trott, O.; McKnight, C. J.; Raleigh, D. P.; Palmer, A. G. *J. Mol. Biol.* **2002**, *320*, 841–854.
- (22) Idiyatullin, D.; Nesmelova, I.; Daragan, V. A.; Mayo, K. H. *J. Mol. Biol.* **2003**, *325*, 149–162.
- (23) Frederick, K. K.; Marlow, M. S.; Valentine, K. G.; Wand, A. *Nature* **2007**, *448*, 325–329.
- (24) Lee, A. L.; Sharp, K. A.; Kranz, J. K.; Song, X.-J.; Wand, A. J. *Biochemistry* **2002**, *41*, 13814–13825.

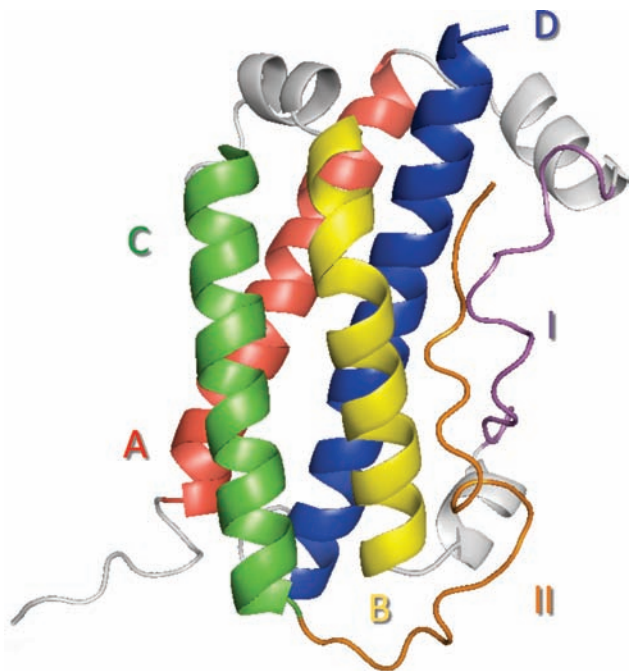


Figure 1. Three-dimensional structure²⁵ of hGH (PDB: 3HHR) showing the four major helices: A, residues 9–34; B, residues 72–92; C, residues 106–128; D, residues 155–184, and the two loop regions, I, residues 48–63, and II, residues 129–154. Three minor helices are included in the structure: one each at the beginning and the end of loop I (residues 38–47 and 64–70, respectively) and one in the short loop between helices B and C (residues 94–100).

dependence observed for the order parameters of most of the backbone amides in the 50–70 °C range, corresponding to local conformational entropies that decrease with temperature and, thus, negative contributions to the local conformational heat capacities.

Here we analyze the temperature dependence of the nanosecond–picosecond dynamics of the backbone amide groups of a structured but locally flexible protein, the acidic form of human growth hormone (hGH), to elucidate the cause of its unusual stability. hGH is a four-helical bundle protein (Figure 1) of ~22 kDa and 191 residues. The X-ray structure of native hGH at pH 5.5 bound to its receptor has been determined²⁵ (PDB: 3HHR). Folding/unfolding studies and NMR studies have indicated that the protein is stable toward both thermal and chemical denaturation over a wide pH range.^{26–29} Between pH 2 and pH 3, hGH populates a state (the acidic form) that is characterized by high backbone flexibility ($S^2_{av} = 0.76 \pm 0.20$) and enhanced NH exchange.²⁹ Yet, the state is stable as judged from a considerable Gibbs free energy of unfolding (30–40 kJ/mol),²⁶ a high temperature of thermal unfolding (~70 °C),²⁸ and preservation of the overall tertiary fold of native hGH.²⁹ However, the high local flexibility

of the acidic form, indicated by the enhanced NH exchange, suggests that the native conformation of the backbone is maintained by a limited number of specific long-range interactions.

Results and Discussion

Temperature Dependent Chemical Shifts. The ¹⁵N and ¹H chemical shifts of the backbone amide groups of hGH as a function of temperature were assigned on the basis of previous assignments at 32 °C, pH 2.65²⁹ (BMRB accession number 4689), as detailed in the Materials and Methods section of the Supporting Information. The ¹H and ¹⁵N chemical shifts are given in Table S1.

Temperature Dependence of the Relaxation and Order Parameters. The ¹⁵N R_1 and R_2 relaxation rates were obtained at 24, 32, 40, and 48 °C and the {¹H}–¹⁵N NOEs at 32, 40, and 48 °C for 104–120 backbone ¹⁵N nuclei in hGH at pH 2.7 (54–63% depending on the temperature). The experimental relaxation parameters are given in Table S2 of the Supporting Information. The NOEs at 24 °C were obtained by linear extrapolation of the values at 32, 40, and 48 °C. The generalized squared order parameters, S^2 , and their temperature derivatives, dS^2/dT , at the four experimental temperatures (Table S3, column 3, and Table S4) were obtained from the relaxation and NOE data by model free calculations, as detailed in the Materials and Methods.

Surprisingly, it is found that the squared order parameter S^2 of many of the residues increases with increasing temperature in the range from 24 °C to about 40 °C, showing that the flexibility of the backbone is decreasing in the regions where the residues are located (see Figure 2 upper four panels). Above ~40 °C, S^2 of these residues decreases, corresponding to an increasing flexibility. For other residues, S^2 decreases continuously with increasing temperature in the entire temperature range (see Figure 2 lower four panels), as normally reported for backbone amide groups in proteins, reflecting an increasing flexibility with increasing temperature.^{14–23} Furthermore, most of the residues with continuously decreasing flexibility are located in the four major helices, while those with increasing flexibility are located in the loops or in the N- or C-terminal, as shown in Figure 3. Moreover, the overall flexibility of the backbones of the four helices decreases almost *concertedly* with temperature up to about 40 °C, while the flexibility of loop II and the C-terminal increases continuously in most of the temperature range from 24 to 48 °C. This is illustrated in Figure 4, which shows the temperature dependence of the average S^2 values for each of the four major helices, the two loops, and the two termini. The overall flexibilities of loop I and the N-terminal are relatively low (relatively large S^2 values) with less uniform temperature variations, probably because of the formation of salt bridges (R8-D11, E32-K41, and E56-K168), as discussed below.

Origin of the Decreasing Helix Flexibility. The decreasing flexibility of the helices in the range from 24 °C to ~40 °C can only be caused by intramolecular interactions that *increase* in strength with increasing temperature. Moreover, the almost concerted decrease of the flexibility of the four helices suggests that the decrease is caused by interactions that involve all four helices. Three kinds of intramolecular interactions can in principle cause the flexibility decrease: hydrogen bonds, hydrophobic interactions, and specific electrostatic interactions (salt bridges) between side chains with opposite charges. Among these, hydrogen bonds will decrease with increasing temperature and can therefore be ruled out. In contrast, hydrophobic

(25) deVos, A. M.; Ultsch, M.; Kossiakoff, A. A. *Science* **1992**, *255*, 306–312.

(26) DeFelippis, M. R.; Kilcomons, M. A.; Lents, M. P.; Youngman, K. M.; Havel, H. A. *Biochim. Biophys. Acta* **1995**, *1247*, 35–45.

(27) Kasimova, M. R.; Milstein, S. J.; Freire, E. *J. Mol. Biol.* **1998**, *277*, 409–416.

(28) Kasimova, M. R. Conformational equilibrium of human growth hormone: a mechanism for the self-association of the intermediate state. Ph.D. Thesis, The Johns Hopkins University, 1999.

(29) Kasimova, M. R.; Kristensen, S. M.; Howe, P. W. A.; Christensen, T.; Matthiesen, F.; Petersen, J.; Sørensen, H. H.; Led, J. *J. Mol. Biol.* **2002**, *318*, 679–695.

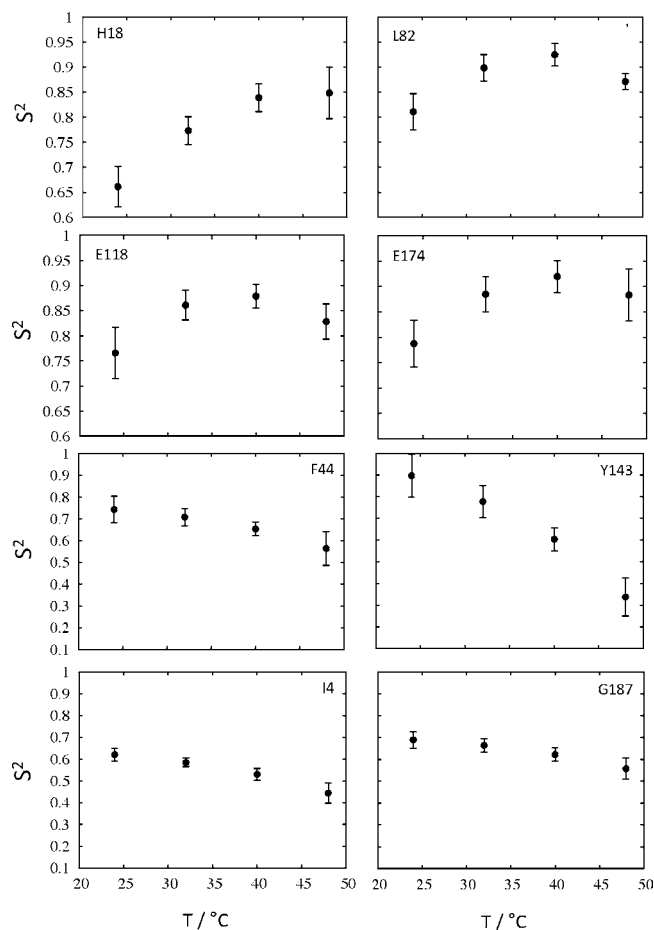


Figure 2. Examples of backbone $^1\text{H}-^{15}\text{N}$ flexibilities of hGH helix residues (H18, A-helix; L82, B-helix; E118, C-helix; E174, D-helix) that decrease (S^2 increase) with increasing temperature in the range from 24 °C to ~40 °C and of hGH loop and terminal residues (F44, loop I; Y143, loop II; I4, N-terminus; G187, C-terminus) that increase (S^2 decrease) with increasing temperature in the entire observed temperature range. Vertical bars indicate one standard deviation.

interactions increase in strength with temperature in the applied temperature range, as shown by Nemethy and Scheraga,³⁰ Baldwin,³¹ and Privalov.³² Since the interior of the four-helix bundle of hGH is almost exclusively made up of hydrophobic side chains,²⁵ hydrophobic interactions may, therefore, contribute to the increasing rigidity of the four helices. Thus, the interior includes the residues F10, A13, L20, and A24 of helix A; L76, S79, I83, W86, and V90 of helix B; V110, L114, L117, I121, and L124 of helix C; and F166, D169, M170, V173, L177, and V180 of helix D. The only two hydrophilic side chains in this list are S79 and D169. However, electrostatic interactions can also contribute to the increasing rigidity of the helices. Thus, as discussed in detail in the following sections, specific interhelical electrostatic interactions in hGH increase in strength with temperature, since the charge of one or more of the interacting groups increases with temperature because of the temperature dependence of the pK_a of the groups.

Identification of Interhelical Salt Bridges. Possible salt bridges were identified on the basis of the distance between oppositely

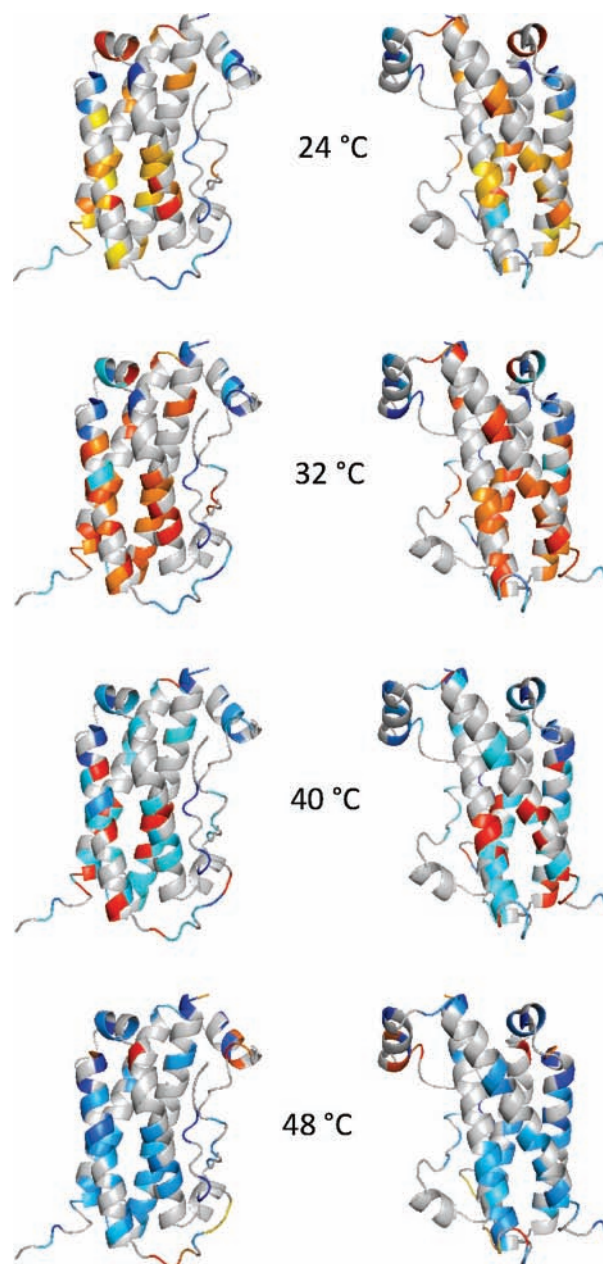


Figure 3. Temperature dependence, dS^2/dT , of the squared order parameters of the observed residues in hGH at 24, 32, 40, and 48 °C. The different colors indicate different values of dS^2/dT : red, $dS^2/dT \geq 0.02$; red \rightarrow yellow, $dS^2/dT = 0.02 \rightarrow 0.00$; cyan \rightarrow blue, $dS^2/dT = 0.00 \rightarrow -0.02$; blue, $dS^2/dT \leq -0.02$. Left panel, front; right panel, back.

charged groups. Following Lounnas and Wade,³³ the distance for defining salt bridges was measured between the centers of the charged groups, defined as follows: C^γ for Asp, C^δ for Glu, N^ζ for Lys, C^ζ for Arg, and N^δ or N^ϵ for doubly protonated His (whichever is closer to the negative residue in the ionic pair). For an ionic pair to be considered a salt bridge, this distance was required to be ≤ 4.8 Å for ionic pairs involving Arg and ≤ 4.3 Å for ionic pairs involving Lys and His. Using these definitions, six salt bridges, H18–E174 (4.25 Å), H21–D171 (3.76 Å), H21–D174 (4.28 Å), R16–D116 (3.97 Å), E32–K41 (4.22 Å), and K115–E118 (3.83 Å) were identified in hGH on the basis of the X-ray structure (Figure 1). Among these,

(30) Nemethy, G.; Scheraga, H. A. *J. Phys. Chem.* **1962**, *66*, 1773–1789.

(31) Baldwin, R. L. *Proc. Natl. Acad. Sci. U.S.A.* **1986**, *83*, 8069–8072.

(32) Privalov, P. L. Physical Basis of the Stability of the Folded Conformations of Proteins. In *Protein Folding*; Creighton, T. F., Ed.; Freeman: New York, 1992; pp 83–126.

(33) Lounnas, V.; Wade, R. C. *Biochemistry* **1997**, *36*, 5402–5417.

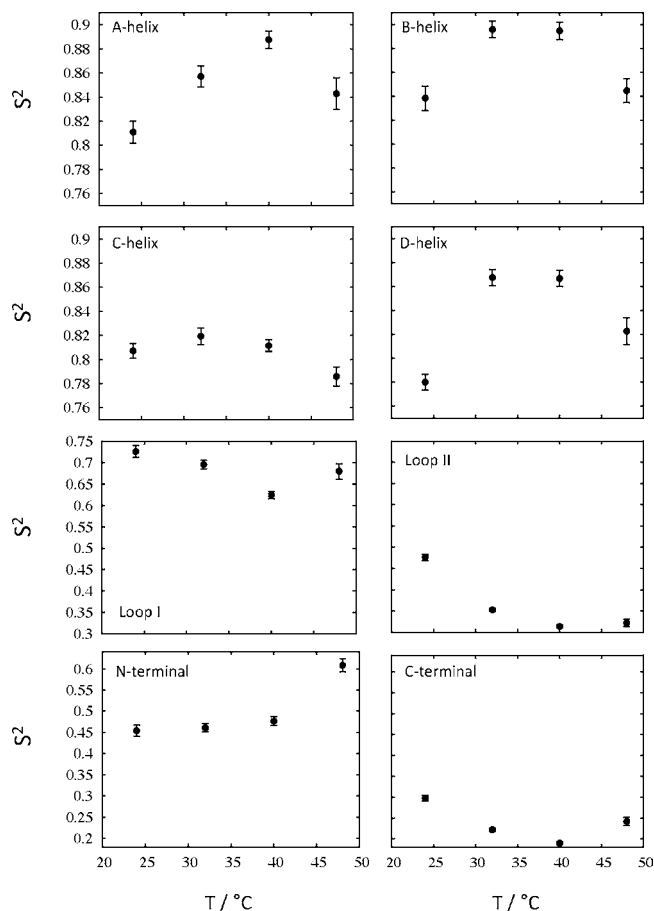


Figure 4. Temperature dependence of the residue-averaged squared order parameters, S^2 , of the backbone ^1H – ^{15}N bond vectors for each of the four major α -helices (A-helix, B-helix, C-helix, and D-helix), the two major loops (loop I and loop II), and the N-terminal residues and C-terminal residues. Vertical bars indicate one standard deviation.

E32–K41 and K115–E118 are between residues that are sequentially close to one another, with the first one connecting the C-terminal end of the A helix with loop I and the second one being *intrahelical* within the C helix. Therefore, both salt bridges can only increase the stability locally and cannot account for the observed overall decrease of the flexibility of the four helices.

In contrast, the four salt bridges H18–E174, H21–D171, H21–E174, and R16–D116 are all *interhelical*, with the first three connecting helix A and D and the last one connecting helix A and C. Figure 5 shows the location of the four salt bridges, all of which are located roughly at the center of the four-helix bundle spatially close to each other, and with the three positively charged residues, R16, H18, and H21, sequentially close in the A helix. Thus, the close-range interhelical electrostatic interactions can form a synergistic network of salt bridges at the center of the four-helix bundle of the hGH molecule that can stabilize the protein and give rise to the observed decreasing flexibility of the helices in the range from 24 °C to ~40 °C.

Confirming the Network of Interhelical Salt Bridges. The pK_a values of the side chains of H18, E174, H21, and D171 and their temperature dependence support the presence of the network of interhelical salt bridges. Thus, the decrease in flexibility of the helices may reflect a strengthening with temperature of the electrostatic interactions between the negatively charged side chain of E174 and the positively charged

imidazole side chains of H18 and H21. Indeed, a titration of the H18 C2H signal³⁴ shows that the residue forms a salt bridge to a group with a pK_a value that *decreases* from 3.39 ± 0.08 at 20 °C to 2.8 ± 0.4 at 32 °C, corresponding to the pK_a values of the E174 carboxyl side chain. In contrast, the pK_a of the H18 imidazole side chain itself *increases* from 7.69 ± 0.02 at 20 °C to 8.16 ± 0.03 at 32 °C. These pK_a values are significantly different from the average pK_a values of 4.2 and 6.6, respectively, reported for glutamic acid and histidine side chains in proteins,³⁵ and they confirm together with their temperature variations that the H18–E174 salt bridge is established and increases in strength with increasing temperature (see below).

Titration of the H21 side chain shows a similar pattern, with two titration shifts corresponding to the titration of an interacting carboxylic side chain and the titration of the H21 imidazole group.³⁴ However, none of the two pK_a values vary in the applied temperature range (2.69 ± 0.14 and 6.62 ± 0.02 , respectively, at 20 °C, and 2.78 ± 0.07 and 6.65 ± 0.03 , respectively, at 32 °C). Still, the histidine side chain is fully charged at the applied pH of 2.7, allowing electrostatic interactions with D171 and E174. The pK_a value of 2.78 ± 0.07 at 32 °C, which is identical to the corresponding pK_a value from the H18 titration (2.8 ± 0.4), indicates that H21 interacts with E174. However, the pK_a value of 2.69 ± 0.14 at 20 °C, which is considerably lower than the corresponding pK_a value from the H18 titration (3.39 ± 0.08), shows that H21 also interacts with another group, which can only be D171 (see Figure 5). A small titration shift of H21 at 32 °C, corresponding to a pK_a value of 8.3 ± 0.3 ,³⁴ indicates that H21 is affected also by the titration of H18.

Hydrophobic Interactions and Salt Bridges Increase in Strength with Temperature. The hydrophobic interactions that dominate the helix core will increase in strength with increasing temperature in the applied temperature range,^{30–32} which may reduce the flexibility of the entire four-helix bundle. However, also the interhelical salt bridges will increase in strength with temperature because of the temperature dependence of the pK_a values of the side chain groups of E174, H18, and H21. At pH 2.7, the ratio of the negatively charged carboxyl group of E174 increases from ~6% to ~44%, when the temperature is raised from 20 to 32 °C, while the histidine side chains of H18 and H21 are fully protonated ($\geq 10^5:1$) and, thus, positively charged at both temperatures. Therefore, the H18–E174 and H21–E174 salt bridges will increase considerably in strength with increasing temperature, reducing the flexibility of the A and D helices. In principle, this would continue until the carboxyl side chain group of the E174 is completely deprotonated. However, the strengthening of both the salt bridges and hydrophobic interactions is counteracted by the increasing thermal energy of the involved side chains and, therefore, reaches a maximum at about 40 °C, according to the experimental results.

The backbone flexibility of the C and B helices decreases almost concertedly with the flexibility of the A and D helices in the temperature range from 24 °C to ~40 °C, as shown by the increase of S^2 observed for most of the residues in the two helices (see Figure 4 and Table S3). In the case of helix C, the R16–D116 salt bridge to helix A may cause part of the decrease. Since the guanidinium group of arginine is fully charged at pH 2.7 ($pK_a \sim 12.5$), the salt bridge can be strengthened only if

(34) Abildgaard, F.; Jørgensen, A. M. M.; Led, J. J.; Christensen, T.; Jensen, E. B.; Junker, F.; Dalbøge, H. *Biochemistry* **1992**, *31*, 8587–8596.

(35) Grimsley, G. R.; Scholtz, J. M.; Pace, C. N. *Protein Sci.* **2009**, *18*, 247–251.

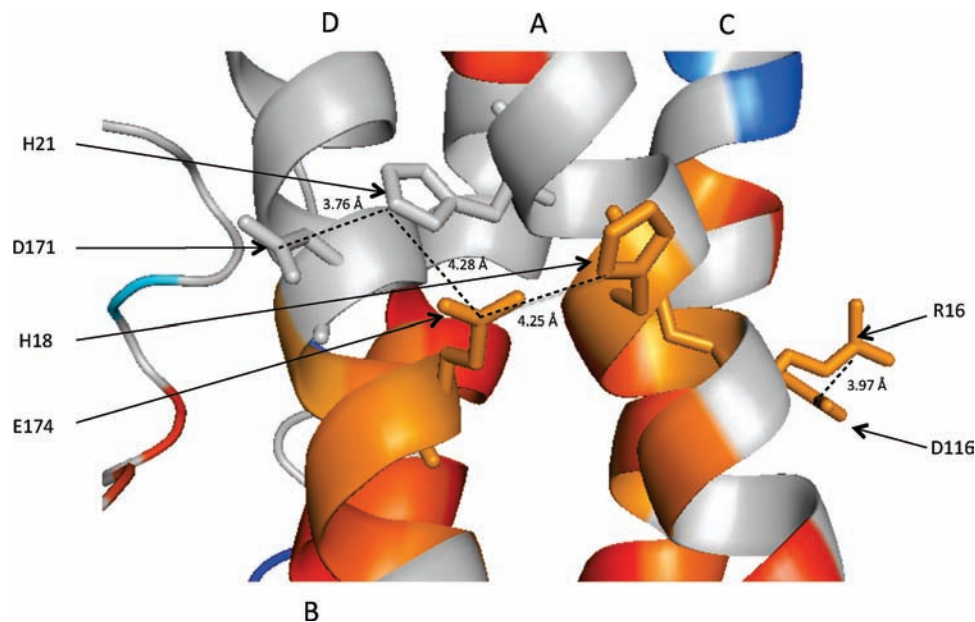


Figure 5. Central part of the core of hGH (Figure 3 at 32 °C) showing the network of salt bridges H18–E174–H21–D171 (from right to left) and the R16–D116 salt bridge (far right) that stabilize the protein at pH 2.7 and increase in strength with increasing temperature in the range from 24 °C to ~40 °C (see text). The helices and the residues involved in the salt bridges are indicated.

the pK_a of D116 decreases with temperature. However, the mere fact that the R16–D116 salt bridge ties the C helix to the rigid A/D helices may decrease its flexibility. Moreover, hydrogen bonding and especially the hydrophobic interactions with the other helices, as discussed above, may reduce the backbone flexibility of the C helix. The decrease of the backbone flexibility of helix B must be caused entirely by its association with the other three helices through the hydrophobic interactions and hydrogen bonding, since none of the residues of the helix participate in interhelical salt bridges.

All in all, the four major helices of hGH are closely tied together by hydrophobic interactions and the network of salt bridges at the center of the four-helix core and possibly by hydrogen bonds. The unusual decrease of the flexibility of the four-helix bundle with increasing temperature must be caused by an increase in strength of the hydrophobic interaction and the salt bridges, with the latter being induced by the decreasing pK_a values, primarily of E174. A determination of the individual contributions from the salt bridges and the hydrophobic interactions could be evaluated by mutations that eliminate the electrostatic interactions. Yet, the fact that only residues involved in or close to the interhelical salt bridges still have an increasing rigidity at 40 °C (Figure 3 and Table S4) indicates that the salt bridges play a prominent role in decreasing the flexibility of the helix backbones and enhancing the stability of the protein with increasing temperature.

The significance of temperature dependent salt bridges for the backbone flexibility of acidic hGH is further emphasized by the effect of the nonhelical salt bridges: R8–D11, E32–K41, and E56–K168. Even though these salt bridges include terminal and loop regions, the flexibility of some of the residues involved in or sequentially close to the salt bridges decreases with increasing temperature at the lower temperatures (see Table S4). For the R8–D11 and E56–K168 salt bridges, this holds even though they are as long as 4.91 Å and 5.46 Å, respectively, in the X-ray structure at pH 5.5.²⁵ However, the average length of the salt bridges here in solution and at the lower pH (2.7) could be different because of a larger mobility of the regions.

Finally, the flexibility of a few residues decreases above ~40 °C, indicating electrostatic interactions that are effective only above this temperature. This, for instance, is the case for D130, G131, and S132 (see Table S4) and could be caused by an E129–R134 salt bridge induced by the temperature dependence of the pK_a value of the side chain carboxyl group of E129.

Backbone Conformational Heat Capacity and the Gibbs Free Energy of Unfolding. The decreasing flexibilities observed for the helix backbones with increasing temperature correspond to decreasing local conformational entropies, S_{conf} (eq 2, Materials and Methods) of the backbone and, thus, a *negative* contribution to the local conformational heat capacities, $C_{p,\text{conf}}$ (eq 3, Materials and Methods). In contrast, the *positive* temperature dependence of the backbone flexibility of most of the loop and terminal residues in the entire temperature range, and of the helix residues above ~40 °C, corresponds to increasing S_{conf} and positive $C_{p,\text{conf}}$ contributions. Typical examples of the two kinds of temperature dependencies are shown in Figure 6. Quantitatively, the actual values of the entropies and heat capacities calculated from eqs 2 and 3 cannot be considered reliable because of the assumptions on which the equations are based^{14,36} and because of the experimental uncertainties (see Figure 6). Still, differences across a protein or between different states of the same protein can provide interesting physical insights. Therefore, a comparison of the $C_{p,\text{conf}}$ values of the backbone amide groups of the individual residues in hGH seems reasonable. Hence, the $C_{p,\text{conf}}$ values of all the observed hGH residues at 24, 32, 40, and 48 °C were estimated from the temperature variation of S^2 , as detailed in the Materials and Methods. The obtained $C_{p,\text{conf}}$ values are given in Table S5.

Primarily, the positive temperature dependence of the backbone flexibilities of the helices above ~40 °C (see Figures 2 and 4) and the positive $C_{p,\text{conf}}$ (see Figure 6) must be caused by the thermal energy of the molecule overcoming the electrostatic and hydrophobic interactions. More interestingly, however, the

(36) Privalov, P. L.; Makhatadze, G. I. *J. Mol. Biol.* **1990**, *213*, 385–391.

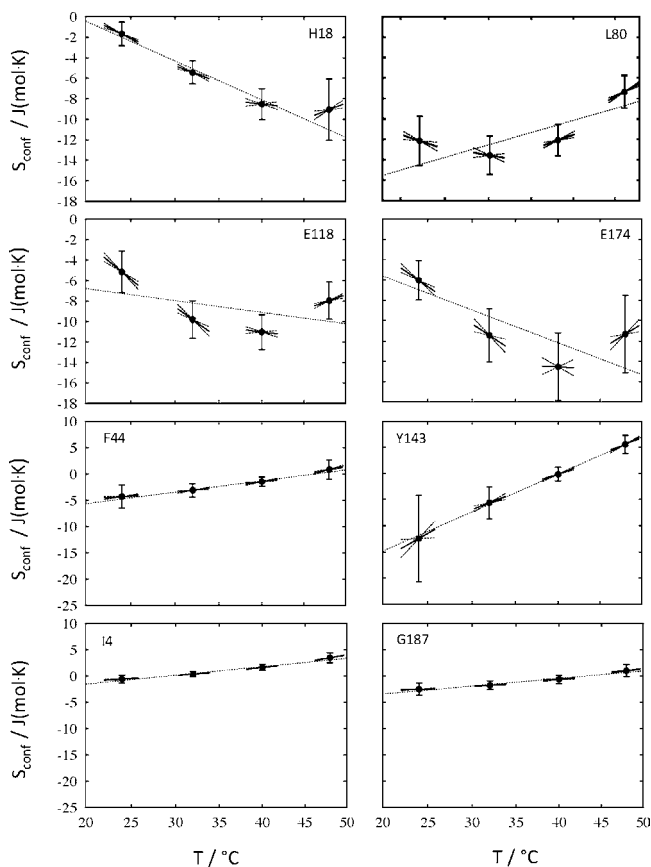


Figure 6. Local conformational entropies, S_{conf} , and heat capacities, $C_{p,\text{conf}}$, versus temperature (natural logarithm scale) of hGH helix residues with negative temperature dependence of the flexibility (H18, A-helix; L80, B-helix; E118, C-helix; E174, D-helix) and of loop and terminal residues with positive temperature dependence of the flexibility (F44, loop I; Y143, loop II; I4, N-terminus; G187, C-terminus). The heat capacities are depicted as the slopes of the entropy (eq 3) with uncertainties (dashed lines). All uncertainties, including those of the entropies (vertical bars), are one standard deviation. The slope of the overall logarithmic least-squares fit to the entropies (straight, through-going dotted lines in the graphs) corresponds to a constant, temperature independent $C_{p,\text{conf}}$.

change in sign of $C_{p,\text{conf}}$ is in accord with the high Gibbs free energy of unfolding (30–40 kJ/mol)²⁶ and the high temperature of unfolding (~ 70 °C) of acidic hGH.²⁸ Thus, the increased rigidity of the helices below ~ 40 °C permits a substantial increase of the flexibility above ~ 40 °C before it reaches the flexibility normally found for helical structures in native proteins.^{18,10} This results in highly positive contributions from the local conformational heat capacities, $C_{p,\text{conf}}$, to the total heat capacity, C_p , of the native protein,⁵⁰ reducing the change in heat capacity upon unfolding, ΔC_p . According to the Gibbs–Helmholtz equation for the temperature dependence of protein stability^{37,38}

$$\Delta G_{\text{unfold}} = \Delta H^* - T\Delta S^* + \Delta C_p [T - T^* - T \ln(T/T^*)] \quad (1)$$

the reduced ΔC_p increases the change in the Gibbs free energy upon unfolding, ΔG_{unfold} , since the temperature term $[T - T^* - T \ln(T/T^*)]$ is negative for $T \leq T^*$. Here, T^* is the convergence temperature, which is approximately 112 °C for

proteins,^{39,38} and ΔH^* and ΔS^* are the enthalpy and entropy changes upon unfolding at T^* and both positive and constant. Thus, the reduced ΔC_p leads to a higher ΔG_{unfold} and, thereby, a higher thermal stability of acidic hGH, in agreement with previous experimental results.^{26–28} Furthermore, the highly positive backbone $C_{p,\text{conf}}$ at temperatures above ~ 40 °C is in agreement with previous observations that the secondary structure regions in more thermostable proteins have relatively high conformational heat capacities.^{18,20,21} Finally, the suggestion here that the interhelical salt bridges can give rise to the reduced ΔC_p and increased thermostability of acidic hGH is in agreement with the experimental observation that salt bridges contribute to the thermostability of a thermophilic protein by reducing its ΔC_p of unfolding.⁴⁰

The discussion above only considers the backbone flexibility, which does not necessarily reflect the dynamics of the side chains. Therefore, inclusion of the flexibility of the side chains would give a more complete picture of the local conformational entropy and its temperature dependence.⁴¹ However, if the side chain flexibility versus temperature follows the same pattern as the backbone flexibility with a minimum value around ~ 40 °C, it will have an effect on ΔG_{unfold} similar to the effect from the backbone flexibility mentioned above. Even if the side chain flexibility should have a different temperature profile, it can hardly cancel the increased contribution to the total C_p from the backbone flexibility, since that would require a negative side chain contribution to C_p above ~ 40 °C; that is, the flexibility of the side chains should decrease above ~ 40 °C. This is highly unlikely, and therefore, the increased backbone $C_{p,\text{conf}}$ above ~ 40 °C can only lead to an increased ΔG_{unfold} of acidic hGH, as discussed above.

Finally, Figure 6 demonstrates the detailed insight provided by the approach used here. Thus, a comparison of the temperature dependent $C_{p,\text{conf}}$ values with the slopes of the straight dotted lines corresponding to constant (temperature independent) $C_{p,\text{conf}}$ values shows that only the approach here reveals the highly positive $C_{p,\text{conf}}$ values above ~ 40 °C and, thereby, the relation between the interhelical interactions (salt bridges and hydrophobic interactions) and the thermostability of acidic hGH, as detailed above.

Reduced Flexibility and Salt Bridges in Nonhelical hGH Regions and in Calmodulin. A positive temperature dependence of S^2 for the backbone amide groups, and, thus, a corresponding negative temperature dependence of S_{conf} and a negative $C_{p,\text{conf}}$, has previously been reported only in a single study.²⁴ This is surprising, considering the occurrence of salt bridges in proteins^{33,42,43} and the results obtained here. The observation of a negative temperature dependence of the local flexibility also in the less structured regions in hGH where the salt bridges R8–D11, E32–K41, and E56–K168 are located suggests that temperature dependent salt bridges may be more common than previously noticed. Indeed, a flexibility that decreases with increasing temperature is found also in Calmodulin. Thus, an analysis of the temperature dependent ^{15}N R_1 and R_2 relaxation

(39) Privalov, P. L. *Adv. Protein Chem.* **1979**, *33*, 167–241.

(40) Lee, C.-F.; Allen, M. D.; Bycroft, M.; Wong, K.-B. *J. Mol. Biol.* **2005**, *348*, 419–431.

(41) Igumenova, T. I.; Frederick, K. K.; Wand, A. J. *Chem. Rev.* **2006**, *106*, 1672–1699.

(42) Kumar, S.; Nussinov, R. *ChemBioChem* **2002**, *3*, 604–617.

(43) Trbovic, N.; Cho, J.-H.; Abel, R.; Friesner, R. A.; Rance, M.; Palmer, A. G., III *J. Am. Chem. Soc.* **2009**, *131*, 615–622.

(37) Becktel, W. J.; Schellman, J. A. *Biopolymers* **1987**, *26*, 1859–1877.
(38) Murphy, K. P.; Privalov, P. L.; Stanley, S. J. *Science* **1990**, *247*, 559–561.

rates and $\{^1\text{H}\}-^{15}\text{N}$ NOEs of Calmodulin⁴⁴ obtained at pH 6.36 and 21 °C, 27 °C, 35 °C, and 43 °C using the approach applied here indicates a temperature dependent flexibility of several of the backbone NH groups similar to what is observed here for hGH, that is, a flexibility and a local conformational entropy that decreases with increasing temperature at lower temperatures and increases at higher temperatures. This includes the four residues with ionizable side chains, K13, E31, R37 and D56 (Figure S1), and suggests that the side chains of these residues are engaged in temperature dependent electrostatic interactions.

Still, it seems surprising if the four residues in Calmodulin are involved in salt bridges, since the relaxation data were recorded at a pH (6.36) significantly different from the average pK_a values found in proteins for the involved ionizable groups. However, as shown in a recent survey of measured pK_a values of ionizable side chains in folded proteins,³⁵ the pK_a values vary considerably, depending on the protein environment in which they are located. Among other things, it was found that the presence of a positively charged environment will lower the pK_a values of all the ionizable groups in a protein, while the presence of a negatively charged environment will raise the pK_a values. Since calmodulin has a large number of negatively charged side chain carboxyl groups, some of the glutamic and aspartic residues (e.g., E31 and D56) could have pK_a values close to the applied pH 6.36.

Thermophilic Proteins. Thermophilic proteins are of particular interest in this context, since they have structural and thermodynamic features similar to those found here for acidic hGH. Thus, most thermophilic proteins have a larger number of salt bridges and a smaller change in heat capacity of unfolding, ΔC_p , than their closest mesophilic homologues.^{40,45,46} Recently, it was demonstrated experimentally in a study of the thermophilic ribosomal protein *T. celer* L30e⁴⁰ that single charge-to-neutral substitutions destabilize the protein by disrupting favorable electrostatic interactions and increasing ΔC_p . Moreover, detailed amide proton exchange studies of the hyperthermophilic protein rubredoxin have shown that the protein has conformational flexibility on the millisecond time scale at ambient temperature ubiquitous throughout the polypeptide chain.⁴⁷ This is in marked contrast to the hypothesis that enhanced thermal stability of hyperthermophilic proteins is the result of increased conformational rigidity in their folded native state,⁴⁸ but in agreement with the enhanced NH exchange of acidic hGH.²⁹ Thus, the structural and thermodynamic characteristics of thermophilic proteins are similar to those found for acidic hGH. It is therefore tempting to suggest that the reduced ΔC_p and the enhanced thermostability of thermophilic proteins are caused by a strengthening with temperature of the salt bridges and that temperature dependent electrostatic interactions are of more general importance for protein stability than appreciated so far, with their exact extent being dependent on the number and the strength of electrostatic interactions in the protein.

Conclusion

All taken together, the results here indicate that the thermostability of hGH at pH 2.7 is caused by interhelical electrostatic

and hydrophobic interactions. The primary effect of these interactions is a negative temperature dependence of the backbone flexibility of the helices below ~ 40 °C and a highly positive temperature dependence above ~ 40 °C, where the thermal energy of the molecule overcomes the electrostatic and hydrophobic interactions. This leads to a reduced heat capacity change of unfolding, ΔC_p , and an increased ΔG_{unfold} and thermostability of hGH. As far as the electrostatic interactions are concerned, these conclusions are supported by a previous study which shows that electrostatic interactions contribute to the thermostability of a thermophilic protein by reducing its ΔC_p of unfolding.⁴⁰ Furthermore, the highly positive backbone $C_{p,\text{conf}}$ above ~ 40 °C, which is found here for the helices in acidic hGH, is in agreement with previous observations that the secondary structure regions in more thermostable proteins have relatively high conformational heat capacities.^{18,20,21} These findings, together with the results presented here, suggest that reduction of ΔC_p by intramolecular interactions, and especially by salt bridges, may be a common mechanism for proteins to achieve thermostability. This may hold, in particular, for thermophilic proteins that are characterized by a larger number of salt bridges and a smaller change in heat capacity of unfolding, ΔC_p , than those for their closest mesophilic homologues.^{40,45,46}

Materials and Methods

The sample preparation, the NMR experiments, and the assignment of the temperature dependent chemical shifts are described in the Materials and Methods section of the Supporting Information.

Theoretical Background. The protein backbone dynamics on the nanosecond–picosecond time scale was determined from NMR relaxation data using the model-free approach,^{1,2} assuming the individual bond vectors diffuse freely within a cone,^{1,3} as detailed in the Materials and Methods section of the Supporting Information. Although more quantitative and elaborate approaches have been proposed,^{12,49} the applied diffusion-in-a-cone model can provide reliable and interesting physical insights into differences across a protein or between different states of the same protein.^{10,14,16–18} Thus, the diffusion-in-a-cone model provides insight into the local flexibility of proteins, primarily in terms of the squared order parameters, S^2 , of backbone N–H bond vectors.

The local conformational entropies, S_{conf} , were derived from the order parameters, S ,^{11,13,14}

$$S_{\text{conf}} = k_B \ln \pi(3 - \sqrt{1 + 8S}) \quad (2)$$

with k_B being the Boltzmann's constant, while the local conformational heat capacities, $C_{p,\text{conf}}$, were obtained from the temperature dependence of S_{conf} ,

$$C_{p,\text{conf}} = \frac{dS_{\text{conf}}}{d \ln T} = T \frac{dS_{\text{conf}}}{dT} \quad (3)$$

with T being the absolute temperature. $C_{p,\text{conf}}$ contributes to the total intrinsic heat capacity, C_p , of the native protein, which includes contributions from all fluctuating covalent and noncovalent interactions within the protein molecule, and protein–solvent interactions.⁵⁰ It is often assumed that C_p is constant within the temperature range sampled.^{14,16} However, as pointed out previously³⁶ and confirmed by the study here, this assumption is not generally correct.

Data Analyses. The temperature derivatives of the backbone ^{15}N R_1 and R_2 relaxation rates and the heteronuclear NOEs were obtained by first fitting a first or second order polynomial (chosen

(44) Chang, S.-L.; Szabo, A.; Tjandra, N. *J. Am. Chem. Soc.* **2003**, *125*, 11379–11384.

(45) Szilágyi, A.; Závodszy, P. *Structure* **2000**, *5*, 493–504.

(46) Petsko, G. A. *Methods Enzymol.* **2001**, *309*, 469–478.

(47) Hernandez, G.; Jenney, F. E.; Adams, M. W. W.; LeMaster, D. M. *Proc. Natl. Acad. Sci. U.S.A.* **2000**, *97*, 3366–3370.

(48) Jaenicke, R.; Böhm, G. *Curr. Opin. Struct. Biol.* **1998**, *8*, 738–748.

(49) Marlow, M. S.; Dogan, J.; Frederick, K. K.; Valentine, K. G.; Wand, A. *J. Nat. Chem. Biol.* **2010**, *6*, 352–358.

by F-statistics) to the experimental relaxation rates and a straight line to the experimental NOEs. From the parameters of the fits, the relaxation rates and NOEs were calculated at T_{exp} (24, 32, 40, and 48 °C) and at $T_{\text{exp}} + 0.1$ K, and the temperature derivatives at T_{exp} were determined as the slopes given by the values at T_{exp} and $T_{\text{exp}} + 0.1$ K. Since corresponding experimental and recalculated relaxation rates and NOEs are within the uncertainties of one another, and since the uncertainties of the recalculated values are more homogeneous and in general smaller than those of the experimental values, the recalculated data were used in the analyses.

The S^2 values were derived from the recalculated relaxation parameters using the model-free approach, as detailed in the Materials and Methods section of the Supporting Information. The model selection was accomplished using standard procedures.⁵¹ To obviate the difficulty of having more free parameters than independent experimental values (^{15}N R_1 and R_2 relaxation rates and NOEs), this procedure expresses the spectral density in five different dynamical regimes, resulting in five models with the following free parameters, model I, S ; model II, S , τ_f ; model III, S , R_{ex} ; model IV, S , τ_f , R_{ex} ; model V, S , S_f , τ_s , where τ_f and τ_s are the internal correlation time for fast and slow motion, respectively, S_f is the generalized order parameter corresponding to τ_f , and R_{ex} represents relaxation caused by motion (exchange) on the slow time scale (μs to ns).

For about one-third of the residues, the model selection procedure chose the same model at all four temperatures. For the rest of the residues, the procedure chose a model with fewer parameters at one or more of the temperatures, often resulting in an S^2 value inconsistent with a continuous temperature dependence of S^2 . However, by imposing the model with the largest number of parameters chosen for a given residue at one of the four temperatures as a common model for the residue at all the temperatures, S^2 values with a continuous temperature dependence were obtained. This also holds for the other parameters determined by the imposed model, although their uncertainties were high in many cases. Interestingly, the NH vectors with internal motion on the 0.3–3 ns time scale (τ_s) are almost exclusively located in loops and terminals, as observed previously.⁸ The number of residues analyzed using the five different models were, model I, 8 residues; model II, 5 residues; model III, 14 residues; model IV, 25 residues; model V, 28 residues. The models used for the individual residues and the obtained model-free parameters are given in Table S3.

(50) Gomez, J.; Hilsner, V. J.; Xie, D.; Freire, E. *Proteins* **1995**, *22*, 404–412.

(51) Mandel, A. M.; Akke, M.; Palmer, A. G., III. *J. Mol. Biol.* **1995**, *246* (1), 144–163.

The S^2 values were derived at each T_{exp} and $T_{\text{exp}} + 0.1$ K, with the latter S^2 values being obtained from the relaxation parameters extrapolated according to their derivatives. The temperature derivatives dS^2/dT were determined as the slope given by S^2 at the two temperatures. Following the same procedure, S_{conf} and dS_{conf}/dT were obtained from S and dS/dT using eq 2. Finally $C_{\text{p, conf}}$ was calculated for each T_{exp} from the obtained dS_{conf}/dT using eq 3.

The overall correlation time, $\tau_m = (2D_{xx} + 2D_{yy} + 2D_{zz})^{-1}$, the rotational diffusion anisotropy, $\eta = 2D_{zz}/(D_{xx} + D_{yy})$, and the direction of the principal component of the rotational diffusion tensor in the molecular frame, given by the polar angles θ and ϕ , were estimated simultaneously from the experimental R_2/R_1 ratios at each temperature, as described previously.²⁹ The overall motional correlation time, τ_m , and the anisotropy, η , varied linearly from 11.9 ± 0.3 ns to 6.7 ± 0.3 ns and from 1.46 to 1.79, respectively, in the applied temperature range (Figure S2), in good agreement with the values 11.9 ns and 1.33 obtained previously at 32 °C.²⁹ The ^{15}N – ^1H bond length and the CSA interaction constant used here were 1.02 Å and -160 ppm, respectively. The statistics of the analysis of the anisotropy of the global tumbling is given in Table S6.

Acknowledgment. We thank Marina R. Kasimova for helpful discussions, Thorkild Christensen, Jørgen Petersen, and Novo Nordisk A/S for providing the ^{15}N labeled human growth hormone used in the study, and Bent O. Petersen for technical assistance. The 800 MHz spectra were acquired at the Danish Instrument Center for NMR Spectroscopy of Biological Macromolecules. The study was supported by the Danish Agency for Science, Technology and Innovation, Grants 21-04-0519, and 272-07-0466.

Supporting Information Available: Chemical shifts of the backbone ^{15}N and ^1H nuclei at ten temperatures from 24 to 48 °C (Table S1) and relaxation data (^{15}N R_1 and R_2 relaxation rates and $\{^1\text{H}\}$ – ^{15}N NOEs) obtained under salt-free conditions at pH 2.7 and 24 °C (except for the NOE), 32 °C, 40 °C, and 48 °C (Table S2), the model-free parameters, including the squared order parameters S^2 versus temperature (Table S3), and dS^2/dT (Table S4) and $C_{\text{p, conf}}$ versus temperature (Table S5) for the individual residues investigated, and the statistics of the analysis of the anisotropy of the global tumbling (Table S6). This material is available free of charge via the Internet at <http://pubs.acs.org>.

JA105388K